Accepted Manuscript

Semidominant Inheritance in Olmsted Syndrome

Xu Cao, Huijun Wang, Yanhong Li, Mingyang Lee, Liya Jiang, Yun Zhou, Cheng Feng, Zhimiao Lin, Yong Yang

PII: S0022-202X(16)31145-9

DOI: 10.1016/j.jid.2016.04.024

Reference: JID 319

To appear in: *The Journal of Investigative Dermatology*

Received Date: 11 January 2016

Revised Date: 28 March 2016

Accepted Date: 28 April 2016

Please cite this article as: Cao X, Wang H, Li Y, Lee M, Jiang L, Zhou Y, Feng C, Lin Z, Yang Y, Semidominant Inheritance in Olmsted Syndrome, *The Journal of Investigative Dermatology* (2016), doi: 10.1016/j.jid.2016.04.024.

Semidominant Inheritance in Olmsted Syndrome

Xu Cao[1,2,3*], Huijun Wang[1,2,3,4*], Yanhong Li[1,2,5], Mingyang Lee[1,2], Liya Jiang[6], Yun Zhou[1,2,7], Cheng Feng[1,2], Zhimiao Lin[1,2†] and Yong Yang[1,2,3†]

[1]Department of Dermatology, Peking University First Hospital, Beijing 100034, China

[2]Beijing Key Laboratory of Molecular Diagnosis on Dermatoses, Beijing 100034, China

[3]Peking-Tsinghua Center for Life Sciences, Beijing 100871, China

[4]Academy for Advanced Interdisciplinary Studies, Peking University, Beijing 100871, China

[5]Department of Dermatology, The Affiliated Hospital of Qingdao University, Qingdao 266003, Shandong Province, China

[6]Department of Dermatology, Liaocheng People's Hospital, Liaocheng 252000, Shandong Province, China

[7]Department of Dermatology, The First Affiliated Hospital of Nanchang University, Nanchang 330006, Jiangxi Province, China

[*]These authors contributed equally to this work.

[†]These authors contributed equally to this work.

Word Counts

Text-1,352, Figure-2, Table-0.

Correspondence: Zhimiao Lin, Department of Dermatology, Peking University First Hospital, Beijing Key Laboratory of Molecular Diagnosis on Dermatoses, Beijing 100034, China; zhimiaolin@bjmu.edu.cn;

Short title: Semidominant Inheritance in OS

Abbreviations: OS, Olmsted syndrome; PPK, palmoplantar keratoderma; TRPV3, transient receptor potential vanilloid type 3;

TO THE EDITOR

Olmsted syndrome (OS; MIM614594) is a hereditary disorder characterized predominantly by palmoplantar keratoderma (PPK) and periorificial keratosis. Frequent additional features include intolerant itching on palms and/or soles, diffuse alopecia, keratosis pilaris, onychodystrophy and digital autoamputation (Mevorah et al., 2005). Recently, mutations in transient receptor potential vanilloid type 3 (*TRPV3*) (Lin et al., 2012) and *MBTPS2* (Haghighi et al., 2013; Wang et al., 2014) have been associated with autosomal-dominant and X-linked OS, respectively. In *TRPV3*-associated OS, we previously demonstrated that certain missense mutations led to over-activation of TRPV3 channel, as an underlying pathogenesis of OS (Lin et al., 2012). In addition to the autosomal-dominant trait, autosomal-recessive OS caused by homozygous or compound heterozygous mutations in *TRPV3* has been described in two families (Duchatelet et al., 2014; Eytan et al., 2014). Herein we report a TRPV3-associated OS family of semidominant inheritance.

The proband was a 6-year-old boy of Chinese Han ethnicity. He was noted to have itchy PPK affecting the weight-bearing areas of his soles at the age of 1 year. At 2 years old, mild keratosis developed on both corners of his mouth and perianal areas. He was diagnosed with OS and was started on oral acitretin 0.5 mg/kg/day. One year later, hyperkeratosis relieved greatly and periorificial keratosis disappeared. Acitretin was then ceased for fear of adverse effects of skeletal abnormality. Hyperkeratosis gradually aggravated to involve his palms with mild flexion contraction of fingers

(Figure 1b and c), while his periorificial areas remained spared. In his fourth year of life, he started to experience paroxysmal burning pain and redness on his distal extremities (Figure 1d). The erythromelalgia was flared by exercise or warmth, relieved after rest or cooling, and became persistent later which required oral carbamazepine to control the symptoms. Four additional family members, including the proband's father, developed asymptomatic, callus-like focal plantar keratosis only on the weight-bearing points with onset ages ranging from 7 to 10 years (Figure 1a, e and Supplementary Figure S1). No mutilation or periorificial keratoderma was found. The proband's mother and sister were phenotypically normal.

We extracted genomic DNA from peripheral blood after written informed consent was obtained in adherence to the Declaration of Helsinki Principles. *TRPV3* coding exons and their flanking regions were amplified and directly sequenced. Two heterozygous mutations, c.1702G>T and c.643+1G>T in *TRPV3* were detected in the proband (Figure 1f and g), which were absent in the 1000 Genome Project, NHLBI ESP, Exome Aggregation Consortium (ExAC) databases, or 200 ethnically-matched normal individuals. Mutation c.643+1G>T was from the mother and c.1702G>T, which led to substitution of glycine by cysteine at position 568 (p.G568C), was of paternal origin and present in all the individuals with plantar keratosis (Figure 1a) and absent in unaffected family members. *In silico* mRNA splicing prediction of mutation c.643+1G>T showed abolishment of the canonical donor splice site of exon 6, which was confirmed by reverse-transcription PCR using RNA extracted from the dorsal

skin of the proband's feet (Supplementary Figure S2 and S3). The results showed that a cryptic donor splice site located at position c.643+2953 was used. Such alternative splicing caused insertion of a 2953-bp intronic sequence downstream of the initiation of intron 6 (Figure 1h and i, Supplementary Figure S3), which resulted in a new premature stop codon p.G215Vfs*82. The same splicing pattern was detected in the mother's skin, but not in normal control skin. To assess the consequence of the splicing mutation, we performed real-time quantitative PCR using the patient skin RNA. Our data showed a reduction of ~50% of total *TRPV3* mRNA in the proband, compared to normal control skin (Supplementary Figure S4), indicating nonsense-mediated mRNA decay.

As the proband exhibited more severe clinical presentation with earlier onset than the other affected individuals harboring one single mutation c.1702G>T, we sought to elucidate the underlying mechanism by assaying the electrophysiological properties of the mutant. We introduced the c.1702G>T mutation at the corresponding site of the human *TRPV3* cDNA, and then inserted either wild-type or mutant cDNA into the pEGFP-N1 plasmid (Clontech, Mountain View, CA). As the TRPV3 channel is a tetramer where four subunits are symmetrically arranged around the ion conduction pore, the subunit composition and functional properties of individual channels vary with TRPV3 allele combinations. We assumed that the proband had only one mutant allele (G568C) expressing TRPV3 subunit, while the other individuals with heterozygous mutation c.1702G>T had equal amount of G568C and wild-type TRPV3

subunits. To mimic the above situations, we recorded currents from HEK293T cells transiently expressing wild-type TRPV3 (WT) or TRPV3-G568C (G568C) separately, or together (WT plus G568C), via the patch-clamp technique as described previously (Cao et al., 2012) (Figure 2a).

First, we tested the voltage-dependent activation of TRPV3 channel which has an important role in TRP channel gating (Voets et al., 2004). When exposed to voltage steps, cells expressing WT showed only small outwardly rectifying currents (Figure 2b), whereas cells expressing WT plus G568C displayed larger outwardly rectifying currents than those expressing WT alone (Figure 2c and e). Remarkably, cells expressing G568C produced the largest outward current with an inactivation-like behavior during depolarization, and had an additional large inwardly rectifying current at negative voltages, implying a constitutively active status at resting membrane potentials (Figure 2d and e). Next, we measured ligand-induced TRPV3 activation by applying 2-aminoethoxydiphenyl borate (2-APB) at concentrations from 1 μM to 1 mM (Figure 2f-h) (Chung et al., 2005). 2-APB activated TRPV3 currents of WT in a concentration-dependent manner with an EC50 value of 65.2 ± 3.4 μM at +80 mV (Figure 2f and i), while WT plus G568C showed a 3-fold EC50 shift of 2-APB-dependent activation, with the EC50 being 19.2 ± 4.5 μM (Figure 2g and i). At an even lower concentration (below 100 μM), 2-APB induced measurable currents in cells transfected with G568C alone, with the EC50 value of 5.7 ± 1.6 μM at +80 mV, which was a more than 10-fold shift of 2-APB-evoked activation (Figure 2h and i).

Previously, it was shown that other *TRPV3* mutations such as G573S or G573C was constitutively active and could not be further activated by 2-APB (Lin *et al.*, 2012; Xiao *et al.*, 2008). Although not as robust as in the mutants at position 573, the activation of G568C was desensitized when the 2-APB concentration reached 1 mM (Figure 2h and i). This phenomenon was only observed when the TRPV3 channel was potently activated (Chung et al., 2005; Hu et al., 2009). Taken together, our results showed that G568C displayed a dramatic gain-of-function property, which could be partially rescued by coassembly with WT subunits.

Semidominant inheritance has been observed in a few genodermatoses, e.g. ichthyosis vulgaris (Smith et al., 2006), pachyonychia congenita (Wilson et al., 2010) and epidermolytic ichthyosis (Nousbeck et al., 2013). Herein we report a case of *TRPV3*-associated OS of semidominant inheritance. We also demonstrated that the clinical severity in the family closely correlated with the electrophysiological properties of the TRPV3 channels. The proband, who is likely to express G568C homomers, showed relatively severe phenotype, while the other affected family members who express WT-G568C heteromers had only mild manifestations, probably due to rescue effects of the WT subunits. This correlation can be supported by significantly more severe, mutilating PPK phenotype (flexion, constriction and autoamputation of digits) caused by TRPV3 G573S or G573C mutations, in which our electrophysiological studies showed constitutively active channel property with insensitivity to 2-APB (Lin *et al.*, 2012).

A recent report of a French family with *TRPV3*-related OS showed that a heterozygous carrier of G568C mutation was clinically normal (Duchatelet et al., 2014a), in contrast to mild, late-onset, focal plantar keratosis in our study. This phenotypic discrepancy indicated factors other than *TRPV3* mutations might also play a role in OS pathogenesis. Our case also developed erythromelalgia, a condition which has been reported elsewhere (Duchatelet *et al.*, 2014a; Duchatelet *et al.*, 2014b). Interestingly, one of two previous cases was compound heterozygous for a splice site mutation and the G568C mutation identified in our patient. Our results further confirmed that certain mutations in *TRPV3* could lead to erythromelalgia in OS patients. Future studies are required to address the association between OS and erythromelalgia in the context of TRPV3 mutations.

Conflict of interest

The authors stated no conflict of interest.

Acknowledgements

We thank the patient and family members who participated in this study. This work was supported by National Natural Science Foundation of China (grant nos. 81201220 to ZL and 81271744 to YY), China National Funds for Distinguished Young Scientists (grant no. 81425020 to YY), China National Funds for Excellent Young Scientists (grant no. 81522037 to ZL), Beijing Nova Program (grant no. Z151100000315044 to ZL) and China Postdoctoral Science Foundation (grant no. 2013T60044 to ZL).

Figure Legend

Figure 1.Clinical features, *TRPV3* mutations and mutant cDNA transcript.

(a) The pedigree of the family. The proband (arrow) with compound heterozygous mutations in *TRPV3* was indicated by black filled symbols, while other mildly affected members were indicated by gray filled symbols.

(b-e) Hyperkeratosis was more severe in the proband (b-d) with flexion contraction of fingers compared to focal plantar keratosis in his father (e). Note the redness on the feet of the proband (d).

(f, g) Genomic DNA sequence of heterozygous mutations c.1702G>T (f) and c.643+1G>T (g) in *TRPV3*. Arrows indicate the mutation nucleotides.

(h) Sequencing of cDNA derived from skin lesion of the proband revealed that mutation c.643+1G>T led to an alternative donor splice site deep in intron 6, resulting in an insertion of 2953 bp from the initiation of intron 6 (termed Exon 6a).

(i) Schematic illustration of the wild-type transcript (WT, top) and the new transcript (bottom) from the allele of mutation c.643+1G>T.

Figure 2.Electrophysiologicalstudies on TRPV3 channels of WT, G568C mutant and WT plus G568C.

(a) Model of TRPV3 channel containing WT subunit (blank), G568C mutant (hatched) and WT plus G568C.

(b-d) Representative inside-out recordings from cells transfected with WT, G568C mutant and WT plus G568C. Patches were held at 0 mV, steps from −160 to 240 mV

in an increment of 20 mV for 300 ms, and then back to −100 for 100 ms.

(e) Respective current density-voltage plots of steady-state currents from b-d.

(f-h) Representative current traces at ± 80 mV were recorded from inside-out patches facing solutions at various concentrations of 2-APB.

(i) 2-APB dose-response curves of WT, G568C mutant and WT plus G568C.

(j) Comparison of EC_{50} values of WT, G568C mutant and WT plus G568C. *n*=3-5. Statistical analyses were performed using Student's *t*-test. **P*<0.05;***P*< 0.01.

.

References:

Cao X, Yang F, Zheng J, Wang K. Intracellular proton-mediated activation of TRPV3 channels accounts for the exfoliation effect of alpha-hydroxyl acids on keratinocytes. J Biol Chem 2012; 287:25905-16.

Chung MK, Guler AD, Caterina MJ. Biphasic currents evoked by chemical or thermal activation of the heat-gated ion channel, TRPV3. J Biol Chem 2005; 280:15928-41.

Duchatelet S, Guibbal L, de Veer S, Fraitag S, Nitschke P, Zarhrate M, et al. Olmsted syndrome with erythromelalgia caused by recessive TRPV3 mutations. Br J Dermatol 2014a; 171:675-8.

Duchatelet S, Pruvost S, de Veer S, Fraitag S, Nitschke P, Bole-Feysot C, et al. A new TRPV3 missense mutation in a patient with Olmsted syndrome and erythromelalgia. JAMA Dermatol. 2014b;150(3):303-6.

Eytan O, Fuchs-Telem D, Mevorach B, Indelman M, Bergman R, Sarig O, et al. Olmsted syndrome caused by a homozygous recessive mutation in TRPV3. J Invest Dermatol 2014; 134:1752-4.

Haghighi A, Scott CA, Poon DS, Yaghoobi R, Saleh-Gohari N, Plagnol V, et al. A missense mutation in the MBTPS2 gene underlies the X-linked form of Olmsted syndrome. J Invest Dermatol 2013; 133:571-3.

Hu H, Grandl J, Bandell M, Petrus M, Patapoutian A. Two amino acid residues determine 2-APB sensitivity of the ion channels TRPV3 and TRPV4. Proc Natl Acad Sci U S A 2009; 106:1626-31.

Lin Z, Chen Q, Lee M, Cao X, Zhang J, Ma D, et al. Exome sequencing reveals mutations in TRPV3 as a cause of Olmsted syndrome. Am J Hum Genet 2012; 90:558-64.

Mevorah B, Goldberg I, Sprecher E, Bergman R, Metzker A, Luria R, et al. Olmsted syndrome: mutilating palmoplantar keratoderma with periorificial keratotic plaques. J Am Acad Dermatol 2005; 53:S266-72.

Nousbeck J, Padalon-Brauch G, Fuchs-Telem D, Israeli S, Sarig O, Sheffer R, et al. Semidominant inheritance in epidermolytic ichthyosis. J Invest Dermatol 2013; 133:2626-8.

Smith FJ, Irvine AD, Terron-Kwiatkowski A, Sandilands A, Campbell LE, Zhao Y, et al. Loss-of-function mutations in the gene encoding filaggrin cause ichthyosis vulgaris. Nat Genet 2006; 38:337-42.

Voets T, Droogmans G, Wissenbach U, Janssens A, Flockerzi V, Nilius B. The principle of temperature-dependent gating in cold- and heat-sensitive TRP channels. Nature 2004; 430:748-54.

Wang HJ, Tang ZL, Lin ZM, Dai LL, Chen Q, Yang Y. Recurrent splice-site mutation in MBTPS2 underlying IFAP syndrome with Olmsted syndrome-like features in a Chinese patient. Clin Exp Dermatol 2014; 39:158-61.

Wilson NJ, Messenger AG, Leachman SA, O'Toole EA, Lane EB, McLean WH, et al. Keratin K6c mutations cause focal palmoplantar keratoderma. J Invest Dermatol 2010; 130:425-9.

Xiao R, Tian J, Tang J, Zhu MX. The TRPV3 mutation associated with the hairless phenotype in rodents is constitutively active. Cell Calcium. 2008;43(4):334-43.

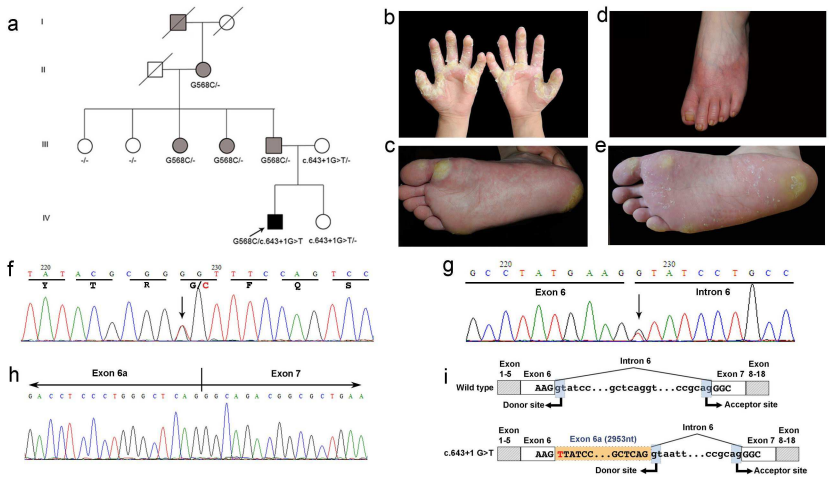

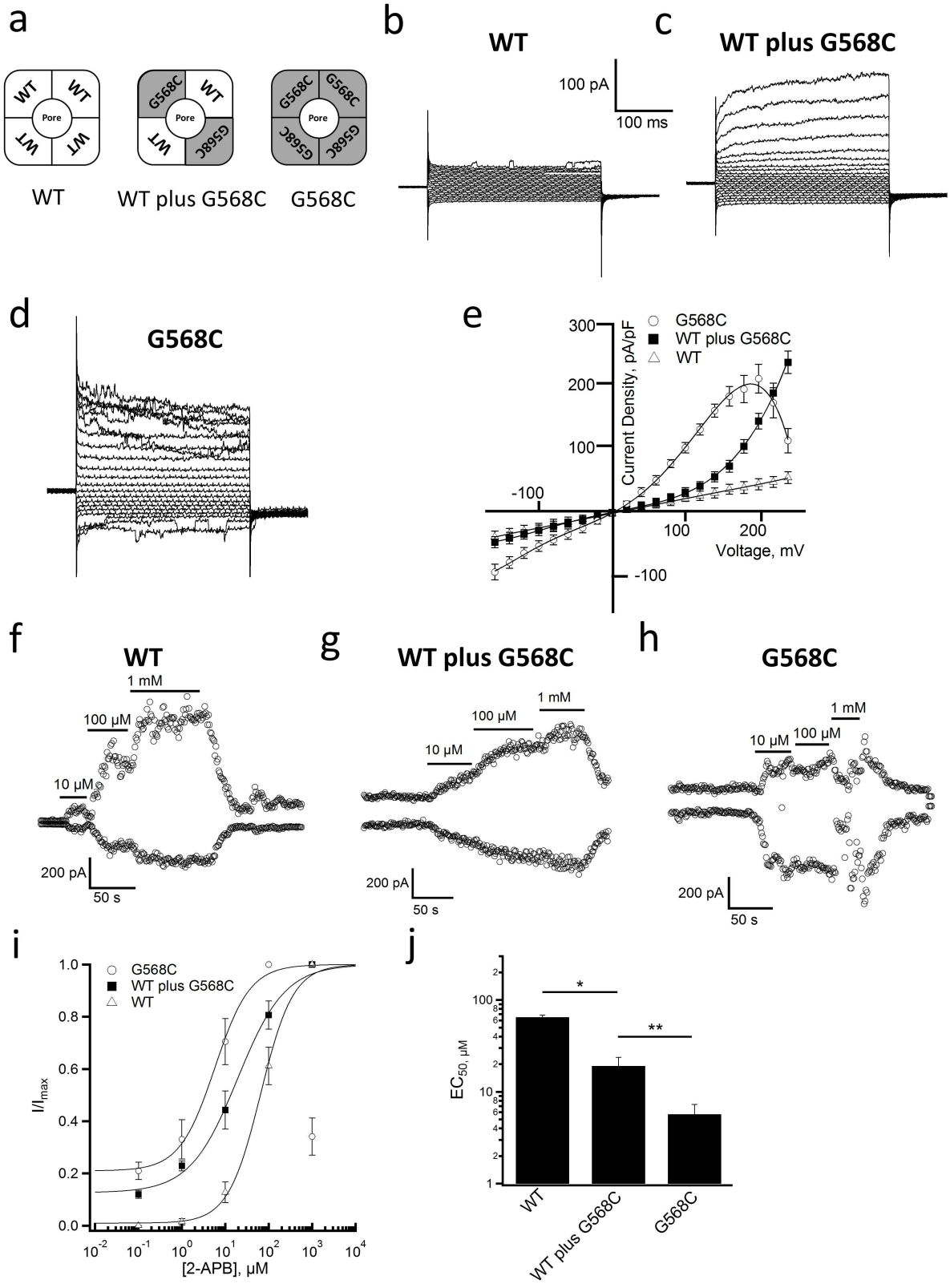
a
WT
WT plus G568C
G568C
Pore
b
WT
100 pA
100 ms
c
WT plus G568C
d
G568C
e
G568C
WT plus G568C
WT
Current Density, pA/pF
Voltage, mV
300
200
100
-100
100
200
-100
f
WT
1 mM
100 µM
10 µM
200 pA
50 s
g
WT plus G568C
1 mM
100 µM
10 µM
200 pA
50 s
h
G568C
1 mM
100 µM
10 µM
200 pA
50 s
i
G568C
WT plus G568C
WT
I/I_max
[2-APB], µM
j
EC50, µM
*
**
WT
WT plus G568C
G568C